Charmed baryon−nucleon interaction

H. Garcilazo,[1,*] A. Valcarce,[2,†] and T. F. Caramés[2,‡]

[1]*Escuela Superior de Física y Matemáticas, Instituto Politécnico Nacional, Edificio 9, 07738 Mexico D.F., Mexico*

[2]*Departamento de Física Fundamental and IUFFyM, Universidad de Salamanca, E-37008 Salamanca, Spain*

(Dated: July 12, 2019)

Abstract

We present a comparative study of the charmed baryon−nucleon interaction based on different theoretical approaches. For this purpose, we make use of i) a constituent quark model tuned in the light-flavor baryon−baryon interaction and the hadron spectra, ii) existing results in the literature based both on hadronic and quark-level descriptions, iii) (2+1)-flavor lattice QCD results of the HAL QCD Collaboration at unphysical pion masses and their effective field theory extrapolation to the physical pion mass. There is a general qualitative agreement among the different available approaches to the charmed baryon−nucleon interaction. Different from hadronic models based on one-boson exchange potentials, quark−model based results point to soft interactions without two-body bound states. They also support a negligible channel coupling, due either to tensor forces or to transitions between different physical channels, $\Lambda_c N - \Sigma_c N$. Short-range gluon and quark-exchange dynamics generate a slightly larger repulsion in the ${}^1S_0$ than in the ${}^3S_1$ $\Lambda_c N$ partial wave. A similar asymmetry between the attraction in the two S waves of the $\Lambda_c N$ interaction also appears in hadronic approaches. A comparative detailed study of Pauli suppressed partial waves, as the ${}^1S_0(I = 1/2)$ and ${}^3S_1(I = 3/2)$ $\Sigma_c N$ channels, would help to disentangle the short-range dynamics of two-baryon systems containing heavy flavors. The possible existence of charmed hypernuclei is discussed.

*Electronic address: humberto@esfm.ipn.mx

†Electronic address: valcarce@usal.es

‡Electronic address: carames@usal.es

I. INTRODUCTION

There has been an impressive experimental progress in the spectroscopy of heavy hadrons, mainly in the charm sector. The theoretical analysis of hidden and open heavy flavor hadrons has revealed how interesting is the interaction of heavy hadrons, with presumably a long-range part of Yukawa type, and a short-range part mediated by quark−quark and quark−antiquark forces. Some of the recently reported states might appear as bound states or resonances in the scattering of two hadrons with heavy flavor content. See Refs. [1–6] for recent overviews and discussions. Thus, the understanding of the baryon−baryon interaction in the heavy flavor sector is a key ingredient in our quest to describing the properties of hadronic matter.

The research programs at various facilities are expected to improve our knowledge on the hadron−hadron interactions involving heavy flavors, particularly in the charm sector. Thus, the LHCb Collaboration at the Large Hadron Collider (LHC) is engaged in an extensive program aimed at the analysis of charmed hadrons produced in the environment of high-energy proton−proton collisions [7]. The observation of five new narrow excited Ω_c states has already been reported [8], some of which are suggested as molecules containing a charmed hadron [1–6]. The planned installation of a 50 GeV high-intensity proton beam at Japan Proton Accelerator Research Complex (J-PARC) [9, 10] intends to produce charmed hypernuclei, in which a Y_c baryon (Λ_c or Σ_c) is bound to a nucleus. There are also planned experiments by the $\overline{\mathrm{P}}$ANDA Collaboration at the Facility for Antiproton Ion Research (FAIR) [11, 12] to produce charmed hadrons by annihilating antiprotons on nuclei.

In addition to the recent interest in the hadron−hadron interaction involving heavy flavors, there is a long history of speculations as regards bound nuclear systems with a charmed baryon. The observation of events that could be interpreted in terms of the decay of a charmed nucleus [13, 14], fostered conjectures about the possible existence of charm analogs of strange hypernuclei [15–17]. This resulted in several theoretical estimates about the binding energy and the potential-well depth of charmed hypernuclei based on one-boson exchange potentials for the charmed baryon−nucleon interaction [18–22]. The current experimental prospects have reinvigorated studies of the low-energy Y_cN interactions [23–32]. See also the recent reviews [33, 34].

As pointed out by Bjorken [35] one should strive to study systems with heavy flavors

because due to their size the quark−gluon coupling constant is small and therefore the leading term in the perturbative expansion is enough to describe the system. However, our ability of making first-principles analytical calculations of nonperturbative QCD phenomena is very limited. When combined with the lack of experimental information on the elementary Y_cN interactions there is room for some degree of speculation in the study of processes involving charmed hadrons. Thus, the situation can be ameliorated with the use of well constrained models based as much as possible on symmetry principles and analogies with other similar processes, which is still a valid alternative for making progress.

Within such a perspective, in this work we present the first comparative study of the charmed baryon−nucleon interaction based on different theoretical approaches. We employ a widely used constituent quark model (CQM) [36, 37] providing a good description of the low-lying spectrum of light and charmed hadrons [38, 39] as well as the nucleon-nucleon interaction [36, 40]. In addition, we consider different scattered results available in the literature. In particular, we compare to the hadronic description based on one-boson exchange potentials of Ref. [26]; the quark-level approach relying on the quark delocalization color screening model (QDCSM) of Ref. [28]; the hybrid model of Ref. [30] based on one-boson exchange potentials supplemented by a global short-range repulsion of quark origin; and the recent charmed baryon−nucleon potential based on a $SU(4)$ extension of the meson-exchange hyperon-nucleon potential $\tilde{A}$ of the Jülich group [41] of Ref. [32]. We will also consider the recent lattice QCD simulations of the Y_cN interactions by the HAL QCD Collaboration [42–45]. However, the lattice QCD simulations are still obtained with unphysical pion masses. They have been extrapolated to the physical pion mass using a chiral effective field theory (EFT) [46].

The paper is organized as follows. In Sect. II we outline the basic ingredients of the CQM used to derive the Y_cN interactions. We also describe the integral equations of the coupled $\Lambda_cN - \Sigma_cN$ system. In Sect. III we present and discuss the results for the Λ_cN and Σ_cN interactions. We show the results of the CQM in comparison to the available results from other theoretical approaches in the literature. We analyze the consequences of the different approaches for the possible existence of charmed hypernuclei. Finally, in Sect. IV we summarize the main conclusions of our work.

II. FORMALISM

A. The quark−quark interaction

The two-body Y_cN interactions are obtained from the chiral constituent quark model of Ref. [36]. The model was proposed in the early 1990s in an attempt to obtain a simultaneous description of the light baryon spectrum and the nucleon-nucleon interaction. It was later on generalized to all flavor sectors [37]. In this model, hadrons are described as clusters of three interacting massive (constituent) quarks. The masses of the quarks are generated by the dynamical breaking of the original $\mathrm{SU}(2)_L \otimes \mathrm{SU}(2)_R$ chiral symmetry of the QCD Lagrangian at a momentum scale of the order of $\Lambda_{\mathrm{CSB}} = 4\pi f_\pi \sim 1$ GeV, where f_π is the pion electroweak decay constant. For momenta typically below that scale, when using the linear realization of chiral symmetry, light quarks interact through potentials generated by the exchange of pseudoscalar Goldstone bosons (π) and their chiral partner (σ):

$$V_\chi(\vec{r}_{ij}) \,=\, V_\sigma(\vec{r}_{ij}) \,+\, V_\pi(\vec{r}_{ij})\,, \tag{1}$$

where

$$V_\sigma(\vec{r}_{ij}) = -\frac{g_{\mathrm{ch}}^2}{4\pi}\,\frac{\Lambda^2}{\Lambda^2 - m_\sigma^2}\,m_\sigma\,\left[Y(m_\sigma\,r_{ij}) - \frac{\Lambda}{m_\sigma}\,Y(\Lambda\,r_{ij})\right]\,,$$

$$\begin{aligned} V_\pi(\vec{r}_{ij}) \,=\, \frac{g_{\mathrm{ch}}^2}{4\pi}\frac{m_\pi^2}{12 m_i m_j}\frac{\Lambda^2}{\Lambda^2 - m_\pi^2} m_\pi \Bigg\{ & \left[Y(m_\pi\,r_{ij}) - \frac{\Lambda^3}{m_\pi^3} Y(\Lambda\,r_{ij})\right]\vec{\sigma}_i\cdot\vec{\sigma}_j \\ & + \left[H(m_\pi\,r_{ij}) - \frac{\Lambda^3}{m_\pi^3} H(\Lambda\,r_{ij})\right] S_{ij}\Bigg\}(\vec{\tau}_i\cdot\vec{\tau}_j)\,. \end{aligned} \tag{2}$$

$g_{\mathrm{ch}}^2/4\pi$ is the chiral coupling constant, m_i are the masses of the constituent quarks, $\Lambda \sim \Lambda_{\mathrm{CSB}}$, $Y(x)$ is the standard Yukawa function defined by $Y(x) = e^{-x}/x$, $H(x) = (1 + 3/x + 3/x^2)\,Y(x)$, and $S_{ij} \,=\, 3\,(\vec{\sigma}_i\cdot\hat{r}_{ij})(\vec{\sigma}_j\cdot\hat{r}_{ij}) \,-\, \vec{\sigma}_i\cdot\vec{\sigma}_j$ is the quark tensor operator.

Perturbative QCD effects are taken into account through the one-gluon-exchange (OGE) potential [47]:

$$V_{\mathrm{OGE}}(\vec{r}_{ij}) = \frac{\alpha_{\mathrm{s}}}{4}\,\vec{\lambda}_i^c\cdot\vec{\lambda}_j^c\left[\frac{1}{r_{ij}} - \frac{1}{4}\left(\frac{1}{2\,m_i^2} + \frac{1}{2\,m_j^2} + \frac{2\vec{\sigma}_i\cdot\vec{\sigma}_j}{3 m_i m_j}\right)\,\frac{e^{-r_{ij}/r_0}}{r_0^2\;r_{ij}} - \frac{3 S_{ij}}{4 m_i m_j r_{ij}^3}\right], \tag{3}$$

where $\vec{\lambda}^c$ are the SU(3) color matrices, $r_0 = \hat{r}_0/\nu$ is a flavor-dependent regularization scaling with the reduced mass ν of the interacting pair, and α_s is the scale-dependent strong coupling

TABLE I: Quark-model parameters.

$m_{u,d}$ (MeV)	313	$g^2_{\rm ch}/(4\pi)$	0.54
m_c (MeV)	1752	m_σ (fm^{-1})	3.42
$\hat{r}_0$ (MeV fm)	28.170	m_π (fm^{-1})	0.70
μ_c (fm^{-1})	0.70	Λ (fm^{-1})	4.2
b (fm)	0.518	a_c (MeV)	230

constant given by [37],

$$\alpha_s(\nu) = \frac{\alpha_0}{\ln\left[(\nu^2+\mu_0^2)/\gamma_0^2\right]}\,, \tag{4}$$

where $\alpha_0 = 2.118$, $\mu_0 = 36.976$ MeV and $\gamma_0 = 0.113$ fm^{-1}. This equation gives rise to $\alpha_{\rm s} \sim 0.54$ for the light-quark sector, $\alpha_{\rm s} \sim 0.43$ for uc pairs, and $\alpha_{\rm s} \sim 0.29$ for cc pairs.

Finally, any model imitating QCD should incorporate confinement. Although it is a very important term from the spectroscopic point of view, it is negligible for the hadron−hadron interaction. Lattice QCD calculations suggest a screening effect on the potential when increasing the interquark distance [48] which is modeled here by,

$$V_{\rm CON}(\vec{r}_{ij}) = -a_c\,(1-e^{-\mu_c\, r_{ij}})\,(\vec{\lambda^c}_i\cdot\vec{\lambda^c}_j)\,, \tag{5}$$

where a_c and μ_c are the strength and range parameters. Once perturbative (one-gluon exchange) and nonperturbative (confinement and dynamical chiral symmetry breaking) aspects of QCD have been incorporated, one ends up with a quark−quark interaction of the form,

$$V_{q_iq_j}(\vec{r}_{ij}) = \begin{cases} [q_iq_j = nn] \Rightarrow V_{\rm CON}(\vec{r}_{ij}) + V_{\rm OGE}(\vec{r}_{ij}) + V_\chi(\vec{r}_{ij}) \\ [q_iq_j = cn/cc] \Rightarrow V_{\rm CON}(\vec{r}_{ij}) + V_{\rm OGE}(\vec{r}_{ij}) \end{cases}\,, \tag{6}$$

where n stands for the light quarks u and d. Notice that for the particular case of heavy quarks (c or b) chiral symmetry is explicitly broken and therefore boson exchanges associated to the dynamical breaking of chiral symmetry do not contribute. The parameters of the model are the ones used for the study of the light one- and two-hadron systems [36–40], and for completeness they are quoted in Table I.

In order to derive the $B_nB_m \to B_kB_l$ interaction from the basic qq interaction defined above, we use a Born−Oppenheimer approximation where the quark coordinates are integrated out keeping R fixed, the resulting interaction being a function of the two-baryon

relative distance. A thorough discussion of the model can be found elsewhere [36, 37, 49]. We show in Fig. 1 the different diagrams contributing to the charmed baryon−nucleon interaction. While diagrams (a) and (b) are considered in a hadronic description, diagrams (c) and (d) correspond to short-range effects due to quark exchanges that are not mapped in a hadronic description. Diagrams (c) and (d) contain one-gluon exchange contributions that are also missed in hadronic models. To illustrate the capability of the model let us just mention how the obtained NN potentials perfectly describe the S wave phase shifts [40].

In the limit where the two baryons Y_cN overlap, the Pauli principle may impose antisymmetry requirements not present in a hadronic description. Such effects, if any, will be prominent for relative S waves, $L = 0$. The S wave normalization kernel of the two-baryon wave function can be written in the overlapping region ($R \to 0$) as [49]

$$\mathcal{N}_{Y_cN}^{L=0SI} \underset{R\to 0}{\longrightarrow} 4\pi \left\{ 1 - \frac{R^2}{8} \left(\frac{5}{b^2} + \frac{1}{b_c^2} \right) \right\} \{ [1 - 3C(S,I)] + ... \} \ , \tag{7}$$

where $C(S,I)$ is a spin−isospin coefficient and b and b_c are the Gaussian parameters for the wave function of the light and charmed quarks, respectively, assumed to be different for the sake of generality. The closer the value of $C(S,I)$ to 1/3 the larger the suppression of the normalization of the wave function at short distances, generating Pauli repulsion [49, 50]. Similarly to Pauli blocked channels, corresponding to $C(S,I)$=1/3, there might exist Pauli suppressed channels, those where $C(S,I)$ is close to 1/3. This is the case for the channels Σ_cN with $(I,J) = (1/2, 0)$ and $(I,J) = (3/2, 1)$ where $C(S,I) = 8/27$ and $7/27$, respectively. The norm kernel gets rather small at short distances giving rise to Pauli repulsion. As we will discuss below, this repulsion will be reflected in the phase shifts. Let us finally note that, although we will discuss the dependence of the results on different values of b_c, we take a reference value of $b_c = 0.5$ fm.

B. The coupled $\Lambda_cN - \Sigma_cN$ system

If we consider the system of two baryons Y_c and N in a relative S state interacting through a potential V that contains a tensor force, then there is a coupling to the Y_cN D wave so

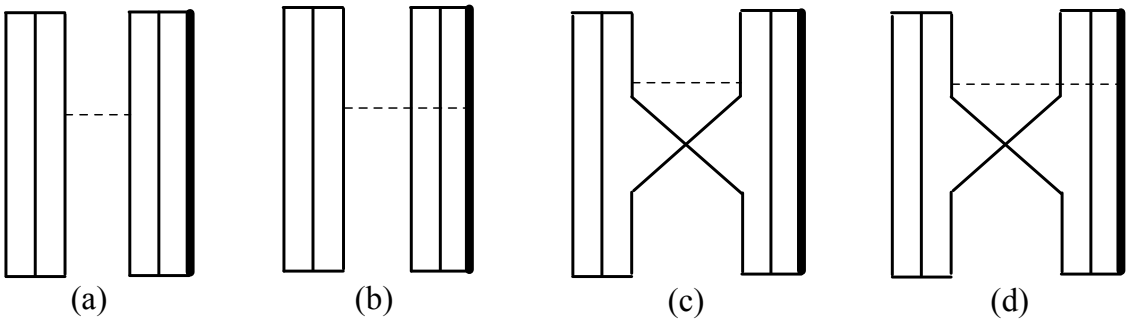

FIG. 1: Representative diagrams contributing to the charmed baryon−nucleon interaction. The vertical solid lines represent a light quark, u or d. The vertical thick solid lines represent the charm quark. The dotted horizontal lines stand for the exchanged boson. (a) Interaction between two light quarks. (b) Interaction between the heavy and a light quark. (c) Interaction between two light quarks together with the exchange of identical light quarks. (d) Interaction between the heavy and a light quark together with the exchange of identical light quarks.

that the Lippmann−Schwinger equation of the system is of the form,

$$t_{JI}^{\ell s \ell'' s''}(p,p'';E) \;=\; V_{JI}^{\ell s \ell'' s''}(p,p'') + \sum_{\ell' s'} \int_0^\infty p'^2 dp'\, V_{JI}^{\ell s \ell' s'}(p,p') \times \frac{1}{E - p'^2/2\mu + i\epsilon} t_{JI}^{\ell' s' \ell'' s''}(p',p'';E)\,, \tag{8}$$

where t is the two-body amplitude, J, I, and E are the total angular momentum, isospin and energy of the system, and ℓs, $\ell' s'$, $\ell'' s''$ are the initial, intermediate, and final orbital angular momentum and spin. p and μ are, respectively, the relative momentum and reduced mass of the two-body system. More precisely, Eq. (8) is only valid for the $\Sigma_c N$ system with isospin 3/2. For this case, the coupled channels of orbital angular momentum and spin that contribute to a given state with total angular momentum J are found in the first two rows of Table II.

In the case of isospin 1/2, the $\Sigma_c N$ states are coupled to $\Lambda_c N$ states. Thus, if we denote the $\Sigma_c N$ system as channel Σ_c and the $\Lambda_c N$ system as channel Λ_c, instead of Eq. (8) the Lippmann−Schwinger equation for $\Lambda_c N - \Sigma_c N$ scattering with isospin 1/2 becomes,

$$t_{\alpha\beta;JI}^{\ell_\alpha s_\alpha \ell_\beta s_\beta}(p_\alpha,p_\beta;E) \;=\; V_{\alpha\beta;JI}^{\ell_\alpha s_\alpha \ell_\beta s_\beta}(p_\alpha,p_\beta) + \sum_{\gamma=\Lambda_c,\Sigma_c} \sum_{\ell_\gamma=0,2} \int_0^\infty p_\gamma^2 dp_\gamma V_{\alpha\gamma;JI}^{\ell_\alpha s_\alpha \ell_\gamma s_\gamma}(p_\alpha,p_\gamma) \times G_\gamma(E;p_\gamma) t_{\gamma\beta;JI}^{\ell_\gamma s_\gamma \ell_\beta s_\beta}(p_\gamma,p_\beta;E); \quad \alpha,\beta = \Lambda_c,\Sigma_c \;, \tag{9}$$

TABLE II: $\Sigma_c N$ channels $(\ell_{\Sigma_c}, s_{\Sigma_c})$ and $\Lambda_c N$ channels $(\ell_{\Lambda_c}, s_{\Lambda_c})$ that contribute to a given state with isospin I and total angular momentum J.

I	J	$(\ell_{\Sigma_c}, s_{\Sigma_c})$	$(\ell_{\Lambda_c}, s_{\Lambda_c})$
3/2	0	(0,0)	
3/2	1	(0,1),(2,1)	
1/2	0	(0,0)	(0,0)
1/2	1	(0,1),(2,1)	(0,1),(2,1)

where $t_{\Sigma_c\Sigma_c;JI}$ is the $\Sigma_c N \to \Sigma_c N$ scattering amplitude, $t_{\Lambda_c\Lambda_c;JI}$ is the $\Lambda_c N \to \Lambda_c N$ scattering amplitude, and $t_{\Sigma_c\Lambda_c;JI}$ is the $\Sigma_c N \to \Lambda_c N$ scattering amplitude. The propagators $G_{\Lambda_c}(E; p_{\Lambda_c})$ and $G_{\Sigma_c}(E; p_{\Sigma_c})$ in Eq. (9) are given by

$$G_\Lambda(E; p_{\Lambda_c}) = \frac{2\mu_{N\Lambda_c}}{k_{\Lambda_c}^2 - p_{\Lambda_c}^2 + i\epsilon}\,, \tag{10}$$

$$G_\Sigma(E; p_{\Sigma_c}) = \frac{2\mu_{N\Sigma_c}}{k_{\Sigma_c}^2 - p_{\Sigma_c}^2 + i\epsilon}\,, \tag{11}$$

with

$$E = k_{\Lambda_c}^2/2\mu_{N\Lambda_c}\,, \tag{12}$$

where the on-shell momenta k_{Σ_c} and k_{Λ_c} are related by

$$\sqrt{m_N^2 + k_{\Lambda_c}^2} + \sqrt{m_{\Lambda_c}^2 + k_{\Lambda_c}^2} = \sqrt{m_N^2 + k_{\Sigma_c}^2} + \sqrt{m_{\Sigma_c}^2 + k_{\Sigma_c}^2}\,. \tag{13}$$

We give in Table II the channels $(\ell_{\Lambda_c}, s_{\Lambda_c})$ and $(\ell_{\Sigma_c}, s_{\Sigma_c})$, corresponding to the $\Lambda_c N$ and $\Sigma_c N$ systems, which are coupled in a given state of total angular momentum J for the case of isospin 1/2.

III. RESULTS AND DISCUSSION

A. $\Lambda_c N$ interaction

We show in Fig. 2(a) the phase shifts for the $\Lambda_c N$ $^1S_0$ partial wave as a function of the center of mass (c.m.) kinetic energy. The latest (2+1)-flavor lattice QCD simulations by the HAL QCD Collaboration [44][1] for a pion mass of 570 (410) MeV are denoted by the

[1] Preliminary studies by the HAL QCD Collaboration of the $\Lambda_c N$ system [42, 43] indicated an extremely weak interaction, while the latest results [44] imply a somewhat stronger though still moderate attractive

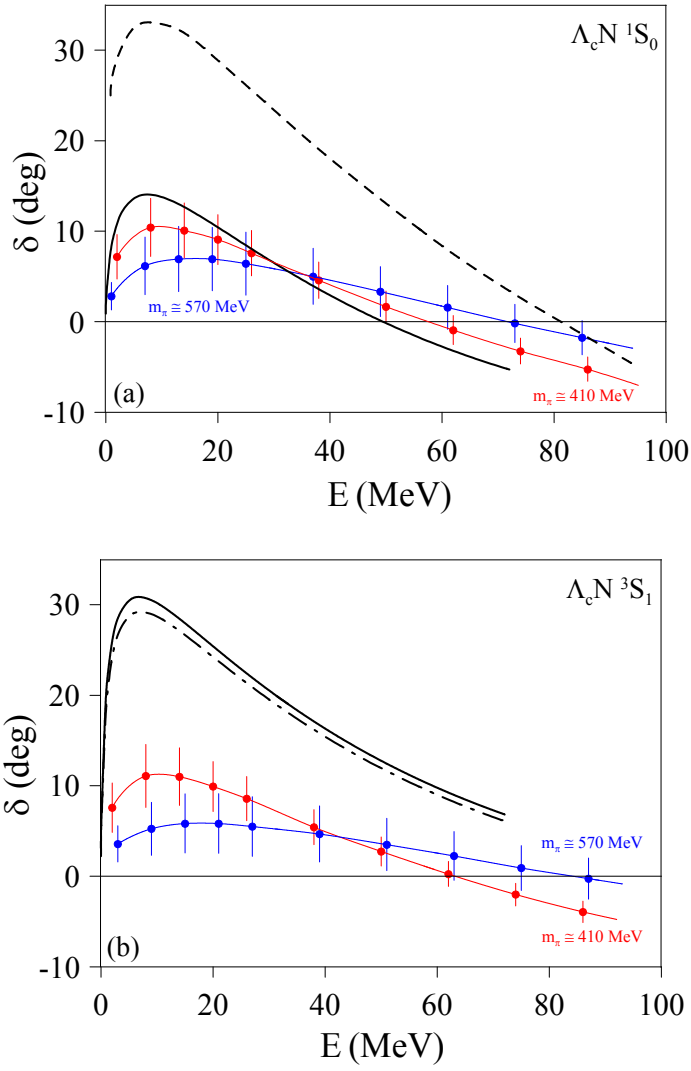

FIG. 2: (a) Phase shifts for the $\Lambda_c N\ ^1S_0$ partial wave as a function of the c.m. kinetic energy. The black solid line stands for the prediction of the CQM. The black dashed line corresponds to the QDCSM results of Ref. [28]. The blue (red) filled circles represent the results of the HAL QCD Collaboration [44] at $m_\pi = 570$ (410) MeV. The vertical line at each point represents the statistical error of the lattice QCD simulations. The solid blue and red lines are just a guide to the eye. (b) Phase shifts for the $\Lambda_c N\ ^3S_1$ partial wave as a function of the c.m. kinetic energy. The black solid line stands for the prediction of the CQM. The black dashed-dotted line represents the CQM phase shifts without channel coupling. The blue (red) filled circles represent the results of the HAL QCD Collaboration [44] at $m_\pi = 570$ (410) MeV. The vertical line at each point represents the statistical error of the lattice QCD simulations. The solid blue and red lines are just a guide to the eye.

interaction.

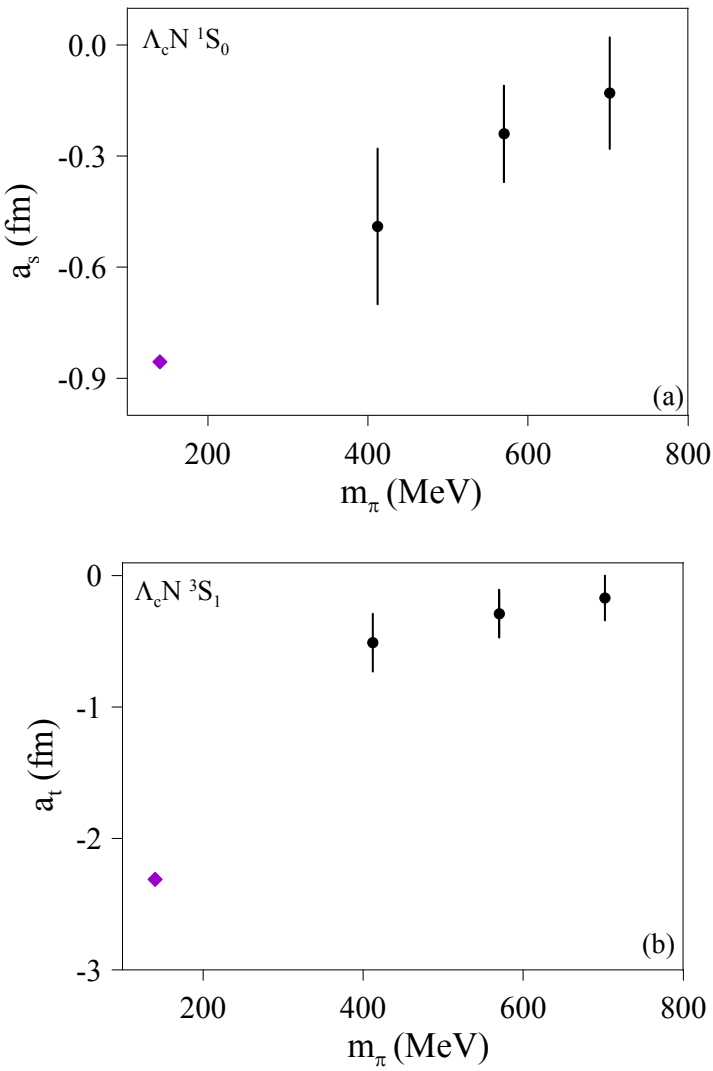

FIG. 3: (a) Dependence of the HAL QCD $\Lambda_c N$ $^1S_0$ scattering length on the pion mass [44]. The vertical bars include statistical and systematic errors. The purple diamond represents the prediction of the CQM for the physical pion mass. (b) Same as (a) for the $\Lambda_c N$ $^3S_1$ partial wave.

blue (red) filled circles with their corresponding errors shown by the vertical lines. The black solid line stands for the results of the CQM described in Sec. II A. The black dashed line corresponds to the results of the QDCSM of Ref. [28] for a color screening parameter $\mu = 0.1$. In Fig. 2(b) we present the phase shifts for the $\Lambda_c N$ $^3S_1$ partial wave — note that in this case the results of the QDCSM model of Ref. [28] are not available. As can be seen there is a tendency that the attraction obtained by the latest lattice QCD simulations for both $\Lambda_c N$ S waves becomes stronger as the pion mass decreases, moving towards the predictions of the CQM and QDCSM models.

In Fig. 3 we show the dependence of the scattering lengths of the spin-singlet and spin-triplet $\Lambda_c N$ partial waves reported by the HAL QCD Collaboration as a function of the pion mass. The purple diamonds at the physical pion mass stand for the results of the CQM. The repulsive or attractive character of the interaction for the different $Y_c N$ partial waves in the CQM is reflected in the scattering lengths and effective range parameters summarized in Table III.

As can be seen in Figs. 2 and 3, the phase shifts and scattering lengths of the $\Lambda_c N$ $^1S_0$ and $^3S_1$ partial waves derived by the HAL QCD Collaboration are qualitatively and quantitatively rather similar. Indeed, it was noted in Ref. [44] that the corresponding $^1S_0$ and $^3S_1$ potentials are almost identical at 410 MeV pion mass and at 570 MeV. These potentials show that the $\Lambda_c N$ interaction is attractive but not strong enough to form two-body bound states. The results of the CQM are slightly different: both partial waves are attractive but without developing two-body bound states. However, the $^3S_1$ partial wave is more attractive than the $^1S_0$. This result is due to the short-range dynamics discussed in Sect. II A, consequence of gluon and quark exchanges. It has been outlined long ago in the literature for the ΛN system [51].

If no meson exchanges were considered, the S wave phase shifts of the $\Lambda_c N$ system are very similar to the corresponding NN scattering [52]. In both partial waves one obtains typical hard-core phase shifts due to the short-range gluon and quark-exchange dynamics. However, the hard-core radius in the spin-singlet state is larger than in the spin-triplet one [51] leading to a more attractive interaction in the spin-triplet partial wave due to a lower short-range repulsion [53]. In fact, the hard cores caused by the color magnetic part of the OGE potential have been calculated in Ref. [51], obtaining 0.35 fm for the spin-triplet state and 0.44 fm for the spin-singlet one. If the short-range dynamics is properly considered, this effect has to be transferred to the phase shifts, as concluded by the CQM. This difference stems from the different expectation value in the spin-singlet and spin-triplet $\Lambda_c N$ partial waves of the color-magnetic operator appearing in Eq. (3), $\vec{\sigma}_i \cdot \vec{\sigma}_j \vec{\lambda}_i^c \cdot \vec{\lambda}_j^c$. The matrix elements of this operator are only different from zero when there are quark-exchange effects, as depicted in diagrams (c) and (d) of Fig. 1[2], giving rise to a genuine quark substructure effect not

[2] If it were not so then there would be net color exchange between two color singlet baryons, which is forbidden by QCD.

TABLE III: CQM results for the $^1S_0$ and $^3S_1$ scattering lengths (a_s and a_t) and effective range parameters (r_s and r_t) in fm for the different Y_cN systems.

I	System	a_s	r_s	a_t	r_t
1/2	Λ_cN	-0.86	5.64	-2.31	2.97
	Σ_cN	$0.74 - i\,0.18$	–	$-5.21 - i\,1.96$	–
3/2	Σ_cN	-1.25	8.70	0.95	4.89

mapped at the hadronic level.

Reference [44] discusses the qualitative difference between the ΛN and Λ_cN interactions due to the absence of K-meson exchanges. The origin of the small spin dependence of the Λ_cN interaction is attributed to the heavy D meson mass and the large separation between the Λ_cN and Σ_cN masses. However, no discussion is found of the role of the short-range dynamics that may contribute to the different behavior of the spin-singlet and spin-triplet Λ_cN phase shifts. As will be discussed below, the short-range dynamics also generates a major impact in the Σ_cN charmed baryon−nucleon interaction. This is due to additional Pauli suppression, as discussed in Sec. II A, in the $^1S_0(I = 1/2)$ and $^3S_1(I = 3/2)$ Σ_cN partial waves, resulting in a strong repulsion.

Recently, Ref. [32] has presented a charmed baryon−nucleon potential based on a $SU(4)$ extension of the meson-exchange hyperon-nucleon potential $\tilde{A}$ of the Jülich group [41]. Three different models of the interaction were considered, which differ only on the values of the couplings of the scalar σ meson with the charmed baryons. In particular, in a first model the couplings of the σ meson with the charmed baryons are assumed to be equal to those of the Λ and Σ hyperons, and their values are taken from the original YN potential $\tilde{A}$ of the Jülich group. In the other two models these couplings are reduced by 15% and 20%, respectively. The Λ_cN phase shifts obtained with these models are in qualitative agreement with the CQM results. They predict a higher overall attraction for the $^3S_1$ than for the $^1S_0$ Λ_cN partial wave, unlike the HAL QCD results, predicting similar phase shifts for both partial waves.

There are other studies of the Y_cN interactions based on one-boson exchange potentials at hadronic level [26, 27]. Although they do not report explicitly phase shifts or scattering lengths, binding energies of the Y_cN two-body systems as a function of the boson-exchange

cutoff Λ_π are calculated. As can be seen in Tables III and IX of Ref. [26] the $J^P = 0^+$ and $J^P = 1^+$ states are bound for any value of Λ_π. The binding energies of the $J^P = 1^+$ state are always a little bit larger than those of the $J^P = 0^+$ state. This is due to the similar contribution of the boson-exchange potentials in both partial waves, the difference coming from the channel coupling that enhances the D wave probability. Thus, while for $\Lambda_\pi = 1.2$ GeV the probability of the $^1S_0$ $\Lambda_c N$ channel in the $J^P = 0^+$ state is 98.2%, that of the $^3S_1$ $\Lambda_c N$ channel in the $J^P = 1^+$ state is 97.6%, with a D wave probability of 1.8%. The small difference between the $^1S_0$ and $^3S_1$ probabilities in the $J^P = 0^+$ and 1^+ states, remains almost constant for any value of Λ_π. For example, for $\Lambda_\pi = 1.6$ GeV they are 80.1% and 79.6%, respectively. However, the D wave probability in the $J^P = 1^+$ state augments from 1.8 to 10.1%. Table IV of Ref. [26] reports binding solutions for the individual channels in the $J^P = 0^+$ state. As can be seen, the uncoupled $^1S_0$ $\Lambda_c N$ state is bound for any value of the cutoff. Unfortunately, binding solutions for the uncoupled $\Lambda_c N$ channel in the $J^P = 1^+$ state are not reported. A simplest guess-by-analogy estimation tells us that the results would be the same in both J^P states if channel coupling was not considered, as happens for the CQM if the short-range dynamics is neglected.

In a later work [30], the hadron level one-boson exchange potential was supplemented by an overall short-range repulsion arising from color-magnetic effects evaluated in the heavy quark limit [54–56]. In general, the results are similar to their previous study, both states $J^P = 0^+$ and $J^P = 1^+$ being bound or at the edge of binding and obtaining larger binding energies in the 1^+ state for the same parametrization. Hence, in both cases [26, 27, 30] one expects phase shifts close to 180 degrees at zero energy, being larger for the spin-triplet partial wave.

The phase shifts for the $^1S_0$ $\Lambda_c N$ interaction reported by the QDCSM model of Ref. [28], dashed line in Fig. 2(a), are more attractive than those of the CQM model, although they do not show a bound state. A major difference between the quark model and hadron level approaches has to do with the strength of the channel coupling. The $\Lambda_c N - \Sigma_c N$ transition is rather weak both in the quark-model description of Ref. [28] and the hadronic or hybrid descriptions of Refs. [26, 27, 30, 32]. However, the tensor effects arising from the pseudoscalar or vector meson exchanges become important at hadronic level[3], while they are negligible

[3] See for example Table III of Ref. [26] where binding energies on the order of hundred MeV are obtained

in the QDCSM study of Ref. [28]. We have calculated the $^3S_1$ $\Lambda_c N$ phase shifts with the CQM just by considering the diagonal interaction. The results are plotted by the dashed-dotted line in Fig. 2(b), where the small contribution of the channel coupling can be seen, in agreement with the QDCSM results of Ref. [28]. It is worth to note that the $\Lambda_c - \Sigma_c$ conversion is less important than in the similar system in the strange sector, mainly due to the larger mass difference, namely 168 MeV as compared to 73 MeV in the strange sector. Besides, it comes reduced as compared to the strange sector due to the absence of K-meson exchanges [20], generating a smaller $\Lambda_c N - \Sigma_c N$ transition potential. The small contribution of the channel coupling obtained by the quark-model descriptions, CQM and QDCSM, to the charmed baryon−nucleon interaction is in agreement with the observations of the HAL QCD Collaboration, leading to the conclusion that the $\Lambda_c N$ tensor potential is negligibly weak [44] and that the coupling between $\Lambda_c N$ and $\Sigma_c N$ channels is also weak [45]. Similar conclusions were obtained in Ref. [32].

Reference [46] has extrapolated the results of the HAL QCD Collaboration to the physical pion mass using EFT. The near-identity of the lattice QCD potentials extracted for the $^1S_0$ and $^3S_1$ $\Lambda_c N$ partial waves [44] persists in the extrapolation to the physical point. As the $^3S_1 - ^3D_1$ tensor coupling induced by the tensor forces is taken into account in the EFT analysis of Ref. [46], it corroborates its smallness in the spin-triplet partial wave, as also derived from the CQM results of Fig. 2(b). The EFT extrapolation to the physical pion mass obtains a maximum for the $^1S_0$ $\Lambda_c N$ phase shift of around 17−21 degrees. This result is compatible with the predictions of the CQM, as seen in Fig. 4(a), where we have calculated the $^1S_0$ $\Lambda_c N$ phase shifts for standard quark-model values of $b_c \in [0.2, 0.8]$ fm. In Fig. 4(b) we have calculated the scattering length for the same interval of values of b_c and we compare with the result of the EFT extrapolation of Ref. [46] at the physical pion mass, the orange vertical line, getting also compatible results. The CQM predicts a slightly larger attraction for the $^3S_1$ $\Lambda_c N$ partial wave. This result, which agrees with the conclusions of Ref. [32], is not expected to coincide with the EFT extrapolation of the HAL QCD $^1S_0$ and $^3S_1$ $\Lambda_c N$ phase shifts, $a_t \in [-0.81, -0.98]$ fm, due to their identity at unphysical pion masses together with the already mentioned smallness of the tensor force in the spin-triplet partial wave.

for the $J^P = 0^+$ $\Lambda_c N$ state with a cutoff $\Lambda_\pi = 1.7$ GeV.

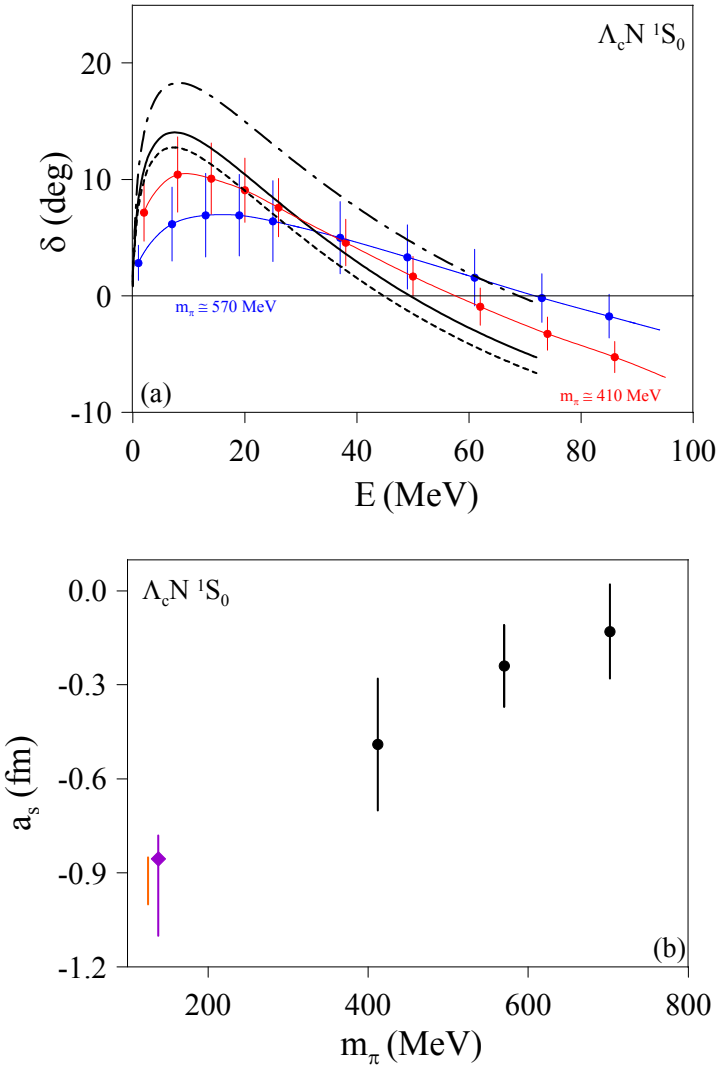

FIG. 4: (a) Phase shifts for the $\Lambda_c N\ ^1S_0$ partial wave as a function of the c.m. kinetic energy. The black solid line stands for the prediction of the CQM for $b_c = 0.5$ fm, the dashed-dotted for $b_c = 0.2$ fm, and the dotted line for $b_c = 0.8$ fm. The blue (red) filled circles represent the results of the HAL QCD Collaboration [44] at $m_\pi = 570$ (410) MeV. The vertical line at each point represents the statistical error of the lattice QCD simulation. The solid blue and red lines are just a guide to the eye. (b) Dependence of the HAL QCD $\Lambda_c N\ ^1S_0$ scattering length on the pion mass [44]. The vertical bars include statistical and systematic errors. The purple diamond represents the prediction for the physical pion mass of the CQM with the uncertainty associated to the range of values of b_c chosen in (a). The orange vertical line stands for the range of values of the EFT extrapolation of Ref. [46] at the physical pion mass.

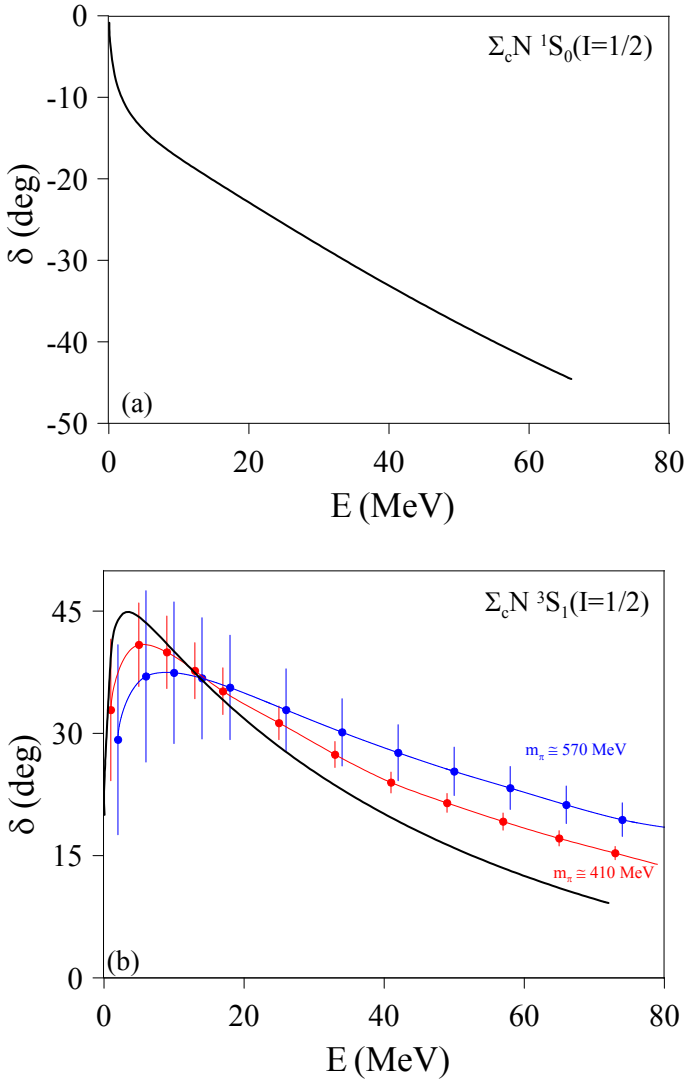

FIG. 5: (a) Phase shifts for the $\Sigma_c N\ ^1S_0(I=1/2)$ partial wave, as a function of the c.m. kinetic energy, predicted by the CQM. (b) Phase shifts for the $\Sigma_c N\ ^3S_1(I=1/2)$ partial wave as a function of the c.m. kinetic energy. The black solid line stands for the prediction of the CQM. The blue (red) filled circles represent the results of the HAL QCD Collaboration [44] at $m_\pi = 570$ (410) MeV. The vertical line at each point represents the statistical error of the lattice QCD simulations. The solid blue and red lines are just a guide to the eye.

B. $\Sigma_c N$ interaction

In Fig. 5 we show the $I = 1/2$ $\Sigma_c N$ phase shifts. Figure 5(a) presents the prediction of the CQM model for the $^1S_0$ partial wave. There are no data available to compare with. The strong repulsion observed in the $\Sigma_c N\ ^1S_0(I=1/2)$ interaction is a consequence of Pauli suppression effects arising in spin−isospin saturated channels [50], as discussed in Sect. II A.

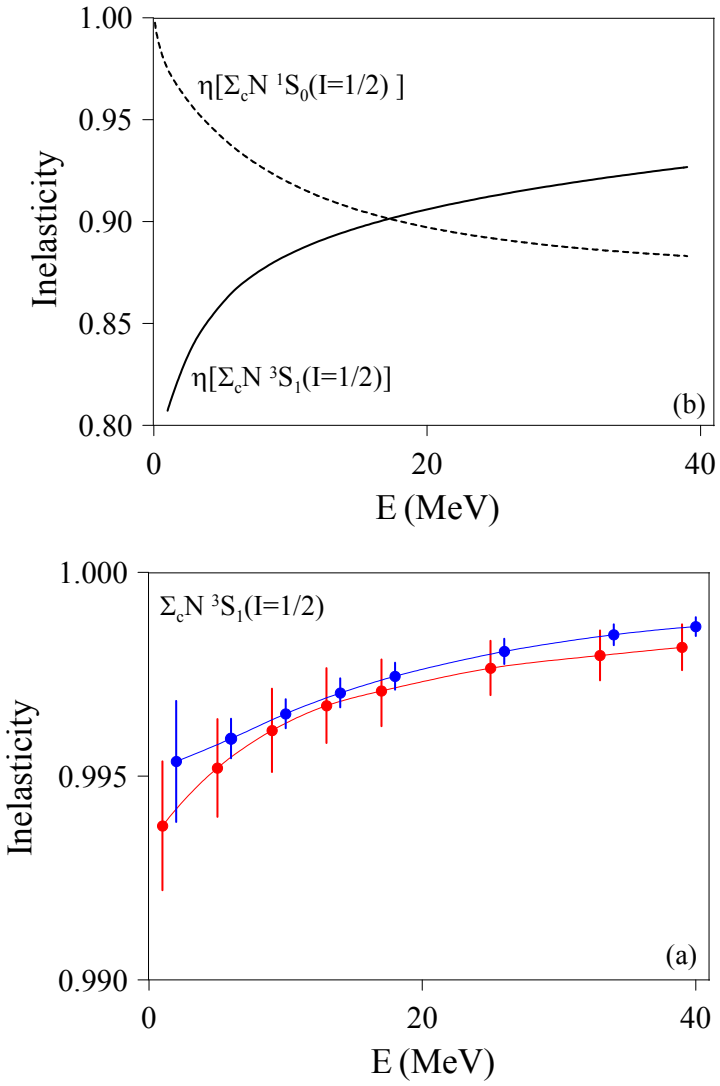

FIG. 6: (a) Inelasticity for the $\Sigma_c N\ ^1S_0(I=1/2)$ and $\Sigma_c N\ ^3S_1(I=1/2)$ partial waves predicted by the CQM as a function of the c.m. kinetic energy. (a) Inelasticity for the $\Sigma_c N\ ^3S_1(I=1/2)$ partial wave of the HAL QCD Collaboration [45] at $m_\pi = 570$ MeV (blue filled circles) and $m_\pi = 410$ MeV (red filled circles) as a function of the c.m. kinetic energy. The vertical line at each point represents the statistical error of the lattice QCD simulations. The solid blue and red lines are just a guide to the eye.

Results of other theoretical approaches for this partial wave would help to disentangle the role of the short-range dynamics in the charmed baryon−nucleon interaction. Figure 5(b) shows the phase shifts for the $^3S_1$ partial wave. The black solid line stands for the results of the CQM. The latest (2+1)-flavor lattice QCD simulations by the HAL QCD Collaboration [44] for a pion mass of 570 (410) MeV are shown by the blue (red) filled circles with their

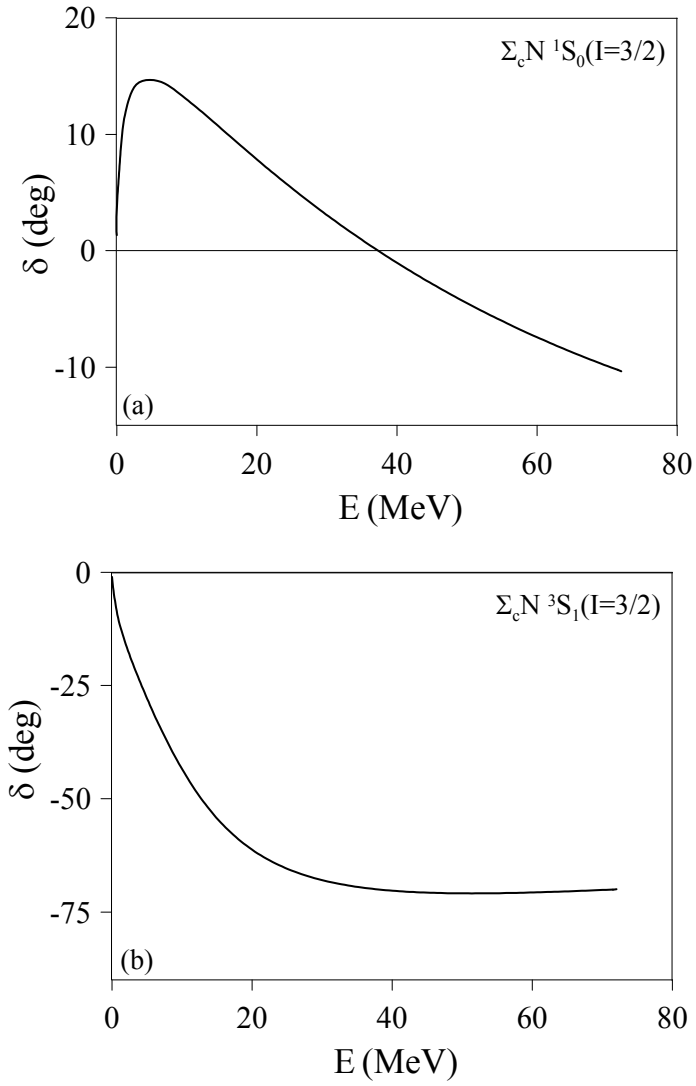

FIG. 7: (a) Phase shifts for the $\Sigma_c N$ $^1S_0(I = 3/2)$ partial wave predicted by the CQM as a function of the c.m. kinetic energy. (b) Same as (a) for the $\Sigma_c N$ $^3S_1(I = 3/2)$ partial wave.

corresponding errors. As in the $\Lambda_c N$ interaction, the tendency can be seen that the attraction becomes stronger as the pion mass decreases, the phase shifts moving towards the results of the CQM. One observes that lattice QCD simulations predict the attraction in the $\Sigma_c N$ $^3S_1(I = 1/2)$ channel to be stronger than in the equivalent $\Lambda_c N$ channel. This conclusion also holds for the CQM results. The attractive or repulsive character of the $\Sigma_c N$ interaction in the CQM is reflected in the scattering lengths given in Table III. Note that the scattering lengths of the $I = 1/2$ $\Sigma_c N$ system are complex because the lower $\Lambda_c N$ channel is always open.

Figure 6(a) shows the inelasticity for the $\Sigma_c N$ $^3S_1(I = 1/2)$ partial wave derived by the HAL QCD Collaboration [45] for a pion mass of 570 (410) MeV by blue (red) filled circles

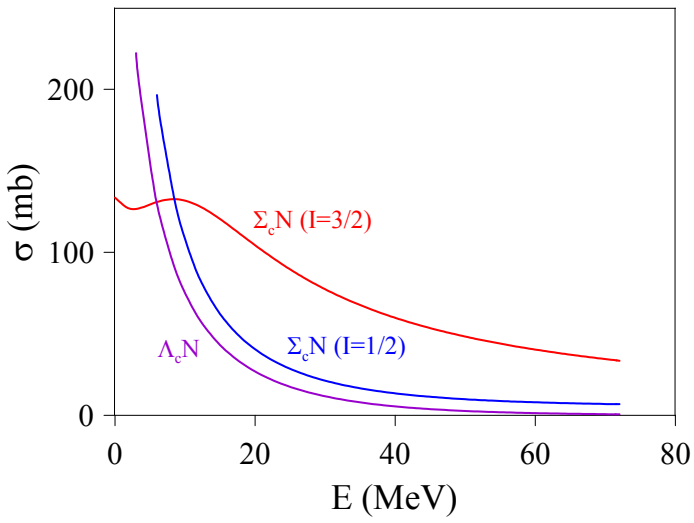

FIG. 8: Total cross section for the $\Lambda_c N$ (purple line), $\Sigma_c N(I = 1/2)$ (blue line) and $\Sigma_c N(I = 3/2)$ (red line) scattering. $E = 0$ stands for the $\Lambda_c N$ or $\Sigma_c N$ thresholds.

with their corresponding errors. Figure 6(b) shows the inelasticity obtained with the CQM for the $\Sigma_c N$ $^3S_1$ and $^1S_0$ $I = 1/2$ partial waves. Although the coupling between the $\Lambda_c N$ and $\Sigma_c N$ channels in the $^3S_1$ partial wave is small, see Fig. 2(b), the inelasticity predicted by the CQM is larger than the HAL QCD simulation.

In Fig. 7 we show the $I = 3/2$ $\Sigma_c N$ phase shifts. The $^1S_0$ $\Sigma_c N$ channel presents an attraction comparable to the $^1S_0$ $\Lambda_c N$ system. The scattering length is still far from the standard values of the ΛN system, in the order of -2.9 to -2.6 fm, which may allow for the existence of three-body bound states as we will discuss below. The $^3S_1(I = 3/2)$ $\Sigma_c N$ channel presents a strong repulsion, a consequence again of quark-Pauli effects arising in spin−isospin saturated channels. As mentioned above for the $\Sigma_c N$ $^1S_0(I = 1/2)$ state, it would be convenient to have results of other theoretical approaches for the phase shifts of the $\Sigma_c N$ $^3S_1(I = 3/2)$ partial wave, to scrutinize the short-range dynamics.

Finally, in Fig. 8 we present the CQM results for the total cross section for the $\Lambda_c N$, $\Sigma_c N(I = 1/2)$, and $\Sigma_c N(I = 3/2)$ scattering.

C. Λ_c hypernuclei.

One of the most interesting applications of the charmed baryon−nucleon interaction is the study of the possible existence of charmed hypernuclei. The binding energy of Λ_c hypernuclei has been analyzed in Ref. [44] using the HAL QCD $\Lambda_c N$ interaction for $m_\pi = 410$ MeV,

where it has been noted that for nuclei with $A = 12 - 58$ the Coulomb repulsion is not much stronger than the strong binding energy, which leads to the possible existence of Λ_c hypernuclei in light or medium−heavy nuclei. On the contrary, Refs. [29, 30] concluded to the existence of light Λ_c hypernuclei. Moreover, Ref. [32] concluded to the existence of Λ_c hypernuclei for all nuclei studied, from ^{5}He to ^{209}Pb.

Regarding the possibility of a $J = 1/2$ charmed hypertriton with the HAL QCD Y_cN interactions there is a delicate balance. On the one hand, it would be favored, bearing in mind the tendency that the Λ_cN attraction becomes stronger as the pion mass decreases. On the other hand, since the average Λ_cN (ΛN) potential that it is relevant for the charmed hypertriton (hypertriton) is dominated by the spin-singlet channel [57], the considerably smaller $^1S_0$ Λ_cN scattering length compared to the ΛN system goes against its existence. The balance could be tilted if the spin dependence of the Λ_cN interaction induced by the short-range dynamics would slightly enhance the attraction in the spin-triplet partial wave as compared with the spin-singlet one. Then, the existence of $J = 3/2$ Λ_c hypernuclei might be considered seriously. The isoscalar $J = 3/2$ state is dominated by the more attractive spin-triplet interaction [58], which together with the reduction of the kinetic energy associated with the Λ_c induced by its larger mass as compared to the Λ, could lead to a slightly bound $J = 3/2$ Λ_c hypernucleus [29]. In this regard, it is important to keep in mind that the isoscalar $J = 3/2$ ΛNN state is close to threshold; see Table V and Fig. 2 of Ref. [59].

The recent few-body calculation of Ref. [30], employing the strongly attractive one-boson exchange interactions discussed above leading already to Λ_cN bound states, leads to several Λ_cNN bound states with binding energies of the order of 20 MeV. As has been discussed above, one made use of a slightly more attractive interaction for the Λ_cN spin-triplet partial wave than for the spin-singlet partial wave. This generates an isoscalar $J = 3/2$ Λ_cNN ground state instead of $J = 1/2$, see Fig. 11 of Ref. [30].

The order of the isoscalar Λ_cNN $J = 1/2$ and $J = 3/2$ channels is also reversed with respect to the strange sector in the CQM model, the $J = 3/2$ being the most attractive one. This difference can easily be associated with the importance of the $\Lambda - \Sigma$ conversion in the strange sector [58]. When the $\Lambda N - \Sigma N$ potential is disconnected, the $J = 3/2$ channel is almost not modified, while the $J = 1/2$ loses great part of its attraction. Thus, the ordering between the $J = 1/2$ and $J = 3/2$ channels is reversed in such a way that the hypertriton would not be bound (see Fig. 6(a) of Ref. [59]). As we have already discussed,

the $\Lambda_c - \Sigma_c$ conversion is less important than in the strange sector, giving rise to a softer $\Lambda_c N - \Sigma_c N$ transition potential. Thus, the calculation of Ref. [29] making use of the CQM phase shifts presented in Figs. 2 and 5, i.e., without two-body bound states, obtained an isoscalar $J = 3/2$ charmed hypernucleus with a binding energy of 0.27 MeV. After correcting exactly by the Coulomb potential the final binding energy obtained was 0.14 MeV. Different from the hadron level calculation of Ref. [30], in the CQM model the $J = 1/2$ $\Lambda_c NN$ is unbound. Let us finally note that the hard-core radius of the $\Lambda_c N$ interaction, relevant for the study of charmed hypernuclei [20], in the CQM is fixed by the short-range dynamics [51].

There are not few-body calculations with the QDCSM $Y_c N$ interactions of Ref. [28]. However, a simple reasoning hints towards the possible existence of a $J = 1/2$ charmed hypertriton in this model. As one can see in Fig. 2(a), the $\Lambda_c N$ $^1S_0$ phase shifts predicted by the QDCSM are similar to those of the $\Lambda_c N$ $^3S_1$ partial wave obtained with the CQM, see Fig. 2(b). As the channel coupling is negligible in both cases, with the QDCSM one would obtain a scattering length for the $\Lambda_c N$ $^1S_0$ state of about -2.31 fm, see Table I. This scattering length is within the order of that of the $^1S_0$ ΛN system, between -2.9 and -2.6 fm, which is a key ingredient for the existence of the hypertriton. The possible existence of a $J = 1/2$ charmed hypertriton in the QDCSM would be reinforced by the reduced kinetic energy contribution of the Λ_c baryon. It might be at an disadvantage by the lack of the $\Lambda N - \Sigma N$ coupling that, as seen in Fig. 6(a) of Ref. [59], is of basic importance to get the hypertriton in quark-model based descriptions.

Reference [32] has also studied the possible existence of bound states of the Λ_c in different nuclei. One makes use of the Λ_c self-energy as an effective Λ_c-nucleus mean-field potential in a Schrödinger equation to get the bound state energies. Λ_c hypernuclei from ${}^{5}_{\Lambda_c}$He to ${}^{209}_{\Lambda_c}$Pb are studied. Even the less attractive model for the $Y_c N$ interaction of those discussed in Sect. III A, where the couplings of the σ meson with the charmed baryons are reduced 20% as compared to the original YN potential $\tilde{A}$ of the Jülich group, is able to bind the Λ_c in all the nuclei considered. This is in contrast with the HAL QCD Collaboration results [44], which suggest that only light- or medium-mass Λ_c nuclei could really exist. The conclusions of this work come to reinforce the results obtained with the CQM in Ref. [29]. On the one hand they arrive at the same conclusion as regards the negligible contribution of the $\Lambda_c N - \Sigma_c N$ coupling, and on the other hand they support the possible existence of light charmed hypernuclei.

IV. OUTLOOK

We have performed a comparative study of the charmed baryon−nucleon interaction based on different theoretical approaches. For this purpose, we make use of i) a constituent quark model tuned in the light-flavor baryon−baryon interaction and the hadron spectra, ii) hadronic descriptions based on one-boson exchange potentials, iii) a quark delocalization color screening model, iv) (2+1)-flavor lattice QCD results of the HAL QCD Collaboration at unphysical pion masses and their effective field theory extrapolation to the physical pion mass. There is a general qualitative agreement among the different available approaches to the charmed baryon−nucleon interaction. Quark-model based results point to soft interactions without two-body bound states. They also support a negligible channel coupling, due either to tensor forces or transitions between different physical channels, $\Lambda_c N - \Sigma_c N$. The short-range dynamics of the CQM model, fixing the hard-core radius of the S wave interactions, generates a slightly larger repulsion in the $^1S_0$ than in the $^3S_1$ $\Lambda_c N$ partial wave. A similar asymmetry between the attraction in the two S waves of the $\Lambda_c N$ interaction also appears in hadronic approaches.

Pauli suppression effects generate a major impact in the $\Sigma_c N$ charmed baryon−nucleon interaction, resulting in a strong repulsion in the $^1S_0(I = 1/2)$ and $^3S_1(I = 3/2)$ partial waves. A comparative detailed study of Pauli suppressed partial waves, as the $^1S_0(I = 1/2)$ and $^3S_1(I = 3/2)$ $\Sigma_c N$ channels, would help to disentangle the short-range dynamics of two-baryon systems containing heavy flavors. Quark-model approaches predict a small contribution of the channel coupling to the charmed baryon−nucleon interaction, concluding that the $\Lambda_c N$ tensor potential is negligibly weak and that the coupling between $\Lambda_c N$ and $\Sigma_c N$ channels is also weak.

In the light of the results for the $Y_c N$ interactions, the possible existence of charmed hypernuclei has been discussed. The order of the isoscalar $J = 1/2$ and $J = 3/2$ channels is reversed in the charm with respect to the strange sector. While the existence of an isoscalar $J = 1/2$ $\Lambda_c NN$ charmed hypernucleus is not likely, that of an isoscalar $J = 3/2$ state seems more feasible. In any case, the possible existence of Λ_c hypernuclei in light or medium−heavy nuclei is a firm prediction of quark-model and hadronic approaches to the $Y_c N$ interaction.

The understanding of the baryon−baryon interaction in the heavy flavor sector is a key ingredient in our quest to describing the properties of hadronic matter. The study of un-

known two-baryon systems could benefit from well-constrained models based as much as possible on symmetry principles and analogies with other similar processes. Subsequently, lattice QCD simulations could incorporate firmly established predictions to validate our understanding of low-energy Quantum Chromodynamics in the multiquark sector.

V. ACKNOWLEDGMENTS

This work has been partially funded by COFAA-IPN (México) and by Ministerio de Economía, Industria y Competitividad and EU FEDER under Contract No. FPA2016-77177-C2-2-P.

[1] Y. -R. Liu, H. -X. Chen, W. Chen, X. Liu, and S. -L. Zhu, Prog. Part. Nucl. Phys. **107**, 237 (2019).

[2] R. A. Briceño *et al.*, Chin. Phys. C **40**, 042001 (2016).

[3] J.-M. Richard, Few-Body Syst. **57**, 1185 (2016).

[4] R. F. Lebed, R. E. Mitchell, and E. S. Swanson, Prog. Part. Nucl. Phys. **93**, 143 (2017).

[5] A. Ali, J. S. Lange, and S. Stone, Prog. Part. Nucl. Phys. **97**, 123 (2017).

[6] A. Esposito, A. Pilloni, and A. D. Polosa, Phys. Rep. **668**, 1 (2017).

[7] S. Ogilvy [LHCb Collaboration], in *Proceedings of the 7th International Workshop on Charm Physics, Detroit (USA)*, SLAC-econf-C1505186 (2015) [arXiv:1509.05611].

[8] R. Aaij *et al.* [LHCb Collaboration], Phys. Rev. Lett. **118**, 182001 (2017).

[9] H. Noumi, JPS Conf. Proc. **17**, 111003 (2017).

[10] H. Fujioka *et al.*, arXiv:1706.07916.

[11] U. Wiedner [$\bar{\text{P}}$ANDA Collaboration], Prog. Part. Nucl. Phys. **66**, 477 (2011).

[12] C. Höhne *et al.*, Lect. Notes Phys. **814**, 849 (2011).

[13] A. A. Tyapkin, Yad. Phys. **22**, 181 (1975). [Sov. J. Nucl. Phys. **22**, 89 (1976)].

[14] Yu. A. Batusov, S. A. Bunyatov, V. V. Lyukov, V. M. Sidorov, A. A. Tyapkin, and V. A. Yarba, JETP Lett. **33**, 52 (1981).

[15] C. B. Dover and S. H. Kahana, Phys. Rev. Lett. **39**, 1506 (1977).

[16] S. Iwao, Lett. Nuovo Cimento **19**, 647 (1977).

[17] R. Gatto and F. Paccanoni, Il Nuovo Cimento A **46**, 313 (1978).

[18] G. Bhamathi, Phys. Rev. C **24**, 1816 (1981).

[19] H. Bandō and M. Bando, Phys. Lett. **109B**, 164 (1982).

[20] H. Bandō and S. Nagata, Prog. Theor. Phys. **69**, 557 (1983).

[21] B. F. Gibson, C. B. Dover, G. Bhamathi, and D. R. Lehman, Phys. Rev. C **27**, 2085 (1983).

[22] N. I. Starkov and V. A. Tsarev, Nucl. Phys. A **450**, 507 (1986).

[23] C. H. Cai, L. Li, Y. H. Tan, and P. Z. Ning, Europhys. Lett. **64**, 448 (2003).

[24] K. Tsushima and F. C. Khanna, J. Phys. G **30**, 1765 (2004).

[25] V. B. Kopeliovich and A. M. Shunderuk, Eur. Phys. J. A **33**, 277 (2007).

[26] Y. -R. Liu and M. Oka, Phys. Rev. D **85**, 014015 (2012).

[27] M. Oka, Nucl. Phys. A **914**, 447 (2013).

[28] H. Huang, J. Ping, and F. Wang, Phys. Rev. C **87**, 034002 (2013).

[29] H. Garcilazo, A. Valcarce, and T. F. Caramés, Phys. Rev. C **92**, 024006 (2015).

[30] S. Maeda, M. Oka, A. Yokota, E. Hiyama, and Y. -R. Liu, Prog. Theor. Exp. Phys. 023D02 (2016).

[31] S. Maeda, M. Oka, and Y. -R. Liu, Phys. Rev. C **98**, 035203 (2018).

[32] I. Vidaña, A. Ramos, and C. E. Jiménez-Tejedor, Phys. Rev. C **99**, 045208 (2019).

[33] A. Hosaka, T. Hyodo, K. Sudoh, Y. Yamaguchi, and S. Yasui, Prog. Part. Nucl. Phys. **96**, 88 (2017).

[34] G. Krein, A. W. Thomas, and K. Tsushima, Prog. Part. Nucl. Phys. **100**, 161 (2018).

[35] J. D. Bjorken, in *Proceedings of the International Conference on Hadron Spectroscopy, Maryland (USA)*, Fermilab Report No. FERMILAB-CONF-85/69 (1985).

[36] A. Valcarce, H. Garcilazo, F. Fernández, and P. González, Rep. Prog. Phys. **68**, 965 (2005).

[37] J. Vijande, F. Fernández, and A. Valcarce, J. Phys. G **31**, 481 (2005).

[38] A. Valcarce, H. Garcilazo, and J. Vijande, Phys. Rev. C **72**, 025206 (2005).

[39] A. Valcarce, H. Garcilazo, and J. Vijande, Eur. Phys. J. A **37**, 217 (2008).

[40] H. Garcilazo, A. Valcarce, and F. Fernández, Phys. Rev. C **60**, 044002 (1999).

[41] A. Reuber, K. Holinde, and J. Speth, Nucl. Phys. A **570**, 543 (1994).

[42] T. Miyamoto [HAL QCD Collaboration], PoS **LATTICE 2015**, 090 (2016).

[43] T. Miyamoto [HAL QCD Collaboration], PoS **LATTICE 2016**, 117 (2017).

[44] T. Miyamoto *et al.* [HAL QCD Collaboration], Nucl. Phys. A **971**, 113 (2018).

[45] T. Miyamoto [HAL QCD Collaboration], PoS **Hadron 2017**, 146 (2018).

[46] J. Haidenbauer and G. Krein, Eur. Phys. J. A **54**, 199 (2018).

[47] A. de Rújula, H. Georgi, and S. L. Glashow, Phys. Rev. D **12**, 147 (1975).

[48] G. S. Bali, Phys. Rep. **343**, 1 (2001).

[49] T. F. Caramés and A. Valcarce, Phys. Rev. D **92**, 034015 (2015).

[50] A. Valcarce, F. Fernández, and P. González, Phys. Rev. C **56**, 3026 (1997).

[51] A. Faessler and U. Straub, Phys. Lett. B **183**, 10 (1987).

[52] A. Valcarce, A. Faessler, and F. Fernández, Phys. Lett. B **345**, 367 (1995).

[53] U. Straub, Z. -Y. Zhang, K. Braüer, A. Faessler, S. B.Khadkikar, and G. Lübeck, Nucl. Phys. A **483**, 686 (1988).

[54] R. L. Jaffe, Phys. Rev. Lett. 38, 195 (1977); 38, 617(E) (1977).

[55] C. Gignoux, B. Silvestre-Brac, and J. -M. Richard, Phys. Lett. B **193**, 323 (1987).

[56] H. J. Lipkin, Phys. Lett. B **195**, 484 (1987).

[57] B. F. Gibson, I. R. Afnan, J. A. Carlson, and D. R. Lehman, Prog. Theor. Phys. Suppl. **117**, 339 (1994).

[58] K. Miyagawa, H. Kamada, W. Glöckle, and V. Stoks, Phys. Rev. C **51**, 2905 (1995).

[59] H. Garcilazo, T. Fernández-Caramés, and A. Valcarce, Phys. Rev. C **75**, 034002 (2007).